

## Transversely modulated crystal structure of charge-orbital ordered manganites $\text{Nd}_{1-x}\text{Sr}_{1+x}\text{MnO}_4$ ( $x = 2/3, 3/4$ )

T. Nagai,<sup>1,3</sup> T. Kimura,<sup>2</sup> A. Yamazaki,<sup>1</sup> T. Asaka,<sup>3</sup> K. Kimoto,<sup>3</sup> Y. Tokura,<sup>2</sup> and Y. Matsui<sup>1,3</sup>

<sup>1</sup>Department of Resources and Environmental Engineering, Waseda University, Tokyo 169-8555, Japan

<sup>2</sup>Department of Applied Physics, University of Tokyo, Tokyo 113-8656, Japan

<sup>3</sup>Advanced Materials Laboratory, National Institute for Materials Science, Tsukuba, Ibaraki 305-0044, Japan

(Received 30 July 2001; published 24 January 2002)

The crystallographic superstructures of the charge-orbital ordered phases were investigated for layered manganites,  $\text{Nd}_{1-x}\text{Sr}_{1+x}\text{MnO}_4$  ( $x = 2/3, 3/4$ ), by high-resolution electron microscopy (HREM) at low temperature. Transverse and sinusoidal structural distortion giving rise to the superstructure were successfully observed in HREM images at 80 K. We also performed the simulations of electron diffraction patterns and HREM images, which support the transverse modulations. The observation implies that a new kind of “Wigner-crystal” model—accompanied with a charge-density wave (CDW) of  $e_g$  electrons—best explains the charge-orbital ordered state in the manganites.

DOI: 10.1103/PhysRevB.65.060405

PACS number(s): 71.45.Lr, 61.14.-x, 68.37.Lp

There has been growing recognition that the interplay of charge, spin, and orbital degrees of freedom should be important for understanding various interesting phenomena in transition-metal oxides, such as metal-insulator transition and colossal magnetoresistance.<sup>1</sup> A number of studies related to the charge-orbital ordering have been performed so far, especially, in perovskite-type manganites. In order to determine real-space ordering patterns of charge and orbital, the crystallographic superstructure has been investigated by diffractometries (x-ray, neutron and electron), transmission electron microscopy, etc.<sup>2–10</sup> Recently, the charge-orbital ordering in  $\text{La}_{1-x}\text{Ca}_x\text{MnO}_3$  ( $x = 2/3$ ) has attracted much attention,<sup>9–12</sup> since there exists the striking discrepancy in the crystallographic superstructures between “Wigner-crystal”<sup>5</sup> and “bi-stripe”<sup>7</sup> models. While longitudinal displacement of atoms was suggested by the “bi-stripe” model, Radaelli *et al.*<sup>9</sup> and Wang *et al.*<sup>10</sup> proposed the “Wigner-crystal” charge-orbital arrangement in which the displacement of atoms is transverse to the modulation wave vector. However, it was difficult to directly observe the transverse modulation in real space mainly because the atomic displacement is very small.<sup>10</sup>

In this paper, we present direct observation of the transverse modulation in charge-orbital ordered manganite crystals,  $\text{Nd}_{1-x}\text{Sr}_{1+x}\text{MnO}_4$  ( $x = 2/3, 3/4$ ), by high-resolution electron microscopy (HREM) at low temperature. The single-layered manganite crystals were found to show charge-orbital ordering transition ( $T_{\text{CO}} \sim 270$  K) in our previous study;<sup>13</sup> these crystals give relatively strong first-order superlattice reflections in electron diffraction, corresponding to long modulation period of  $6d_{110}$  ( $x = 2/3$ ) or  $8d_{110}$  ( $x = 3/4$ ). From this observation, we deduce that, below  $T_{\text{CO}}$ , the crystals of  $\text{Nd}_{1-x}\text{Sr}_{1+x}\text{MnO}_4$  ( $x = 2/3, 3/4$ ) undergo a sinusoidal transverse modulation so as to arrange as far apart as possible for most distorted  $\text{MnO}_6$  stripes and have the crystallographic superstructures consistent with both the Wigner-crystal charge-orbital arrangement and a charge-density wave (CDW) of  $e_g$  electrons.

Single crystalline samples of  $\text{Nd}_{1-x}\text{Sr}_{1+x}\text{MnO}_4$  were melt-grown by the floating-zone method. HREM observation

was conducted with a Hitachi HF-3000 field-emission transmission electron microscope, equipped with a low-temperature sample holder (Oxford Instruments), and operated at 300 kV. The HREM specimens were prepared by crushing the single crystals. Image simulations based on dynamic electron-diffraction theory were carried out with MacTempas software.

The formation of superstructure accompanied by charge-orbital ordering is revealed by the appearance of additional superlattice reflections in the electron diffraction pattern below  $T_{\text{CO}}$  ( $\sim 270$  K) in the present  $\text{Nd}_{1-x}\text{Sr}_{1+x}\text{MnO}_4$  ( $x = 2/3, 3/4$ ) crystals. Figure 1 shows [001] zone-axis diffraction patterns obtained (a) at 300 K for  $x = 2/3$ , (b) at 80 K for  $x = 2/3$ , and (c) at 80 K for  $x = 3/4$ . The patterns obtained at 300 K for both the  $x = 2/3$  and  $x = 3/4$  crystals are indexed

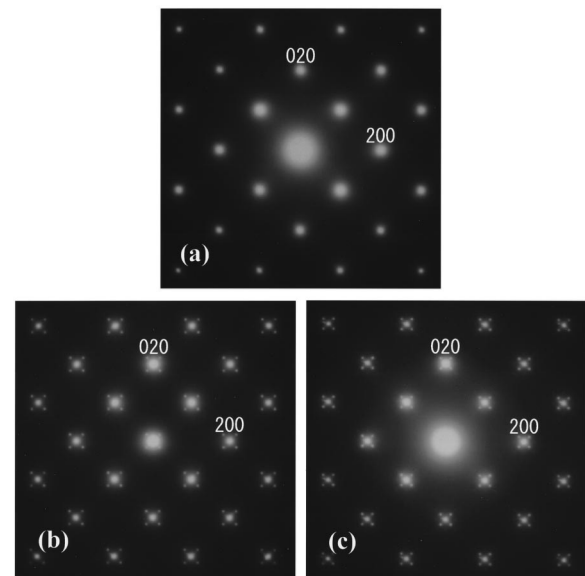


FIG. 1. [001] zone-axis diffraction patterns of  $\text{Nd}_{1-x}\text{Sr}_{1+x}\text{MnO}_4$  crystals (a) at 300 K for  $x = 2/3$ , (b) at 80 K for  $x = 2/3$ , and (c) at 80 K for  $x = 3/4$ . [The pattern at 300 K for  $x = 3/4$  is almost identical to (a).] The presence of superlattice reflections at low temperature is evident.

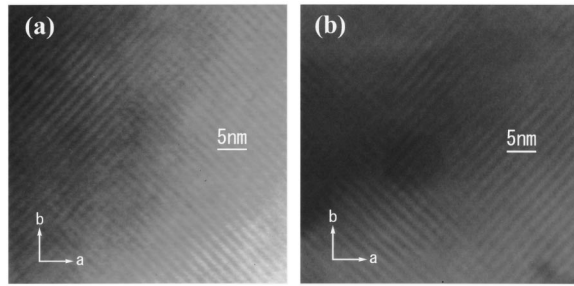


FIG. 2. Lattice images taken at 80 K along the [001] direction for (a)  $x=2/3$  and (b)  $x=3/4$ , showing the superlattice fringes with the period of  $6d_{110}$  ( $x=2/3$ ) or  $8d_{110}$  ( $x=3/4$ ).

with  $I4/mmm$  tetragonal structure ( $K_2NiF_4$  type structure) with  $a=0.3832$  nm,  $c=1.2368$  nm ( $x=2/3$ ),  $a=0.3821$  nm,  $c=1.2380$  nm ( $x=3/4$ ). It is clearly visible that diffraction patterns taken at 80 K show a series of sharp, strong satellite spots around the fundamental Bragg reflections. The satellite spots reflect a modulation giving rise to superstructure. The wave vector of this structural modulation can be described as  $\mathbf{q}=\mathbf{a}^*[1/6,\pm 1/6,0]$  ( $\mathbf{a}\cdot\mathbf{a}^*=1$ ) for  $x=2/3$ , and  $\mathbf{q}=\mathbf{a}^*[1/8,\pm 1/8,0]$  for  $x=3/4$ . Upon cooling from room temperature, the weak satellite reflections appear around 270 K, and the intensity of the reflections increases progressively with decreasing temperature. Around 270 K, both crystals exhibit anomalous behaviors implying charge-orbital ordering transition, such as a steep rise of resistivity with current parallel to the  $MnO_2$  layers<sup>15</sup> and a suppression of magnetic susceptibility toward lower temperatures.

The observed superlattice patterns are indicative of the  $d_{3x^2-r^2}/d_{3y^2-r^2}$  orbital ordering of  $Mn^{3+}$  accompanied by the real-space ordering of  $Mn^{3+}/Mn^{4+}$  species along the diagonal direction in the  $a$ - $b$  plane, which has been observed for other charge-orbital ordered manganites.<sup>3,5,6,14</sup> We now determine the basic characteristics of the superstructure modulation. Figure 2 shows the lattice images taken at 80 K along the [001] direction for (a)  $x=2/3$  and (b)  $x=3/4$ . It can be seen that the charge-orbital ordered crystals consist of domains with one-dimensional modulation along the [110] or  $[1\bar{1}0]$  direction, and that the superlattice reflections showing [110] modulation and those showing  $[1\bar{1}0]$  modulation in the electron diffraction come from the different areas of the crystals. It was also found that the superlattice spots at the positions  $(h,h,0)\pm m(1/6,1/6,0)$  for  $x=2/3$ , or  $(h,h,0)\pm m(1/8,1/8,0)$  for  $x=3/4$ , disappear when the crystal is tilted far away from the [001] zone axis. This observation indicates that the superlattice reflections in the  $(110)^*$  section of the reciprocal space are caused by the multiple scattering of the electron beam, and that local areas of the crystal have slight deviation from the exact [001] zone axis orientation when the pattern shown in Fig. 1 (b) or (c) is observed. The absence of superlattice reflections in the  $(110)^*$  section is suggestive of lattice distortion transverse to the [110], the direction of the modulation.

In order to clarify the superstructure modulation, we observed the high-resolution superstructure images. Figure 3 shows the high-resolution images taken along the [001] di-

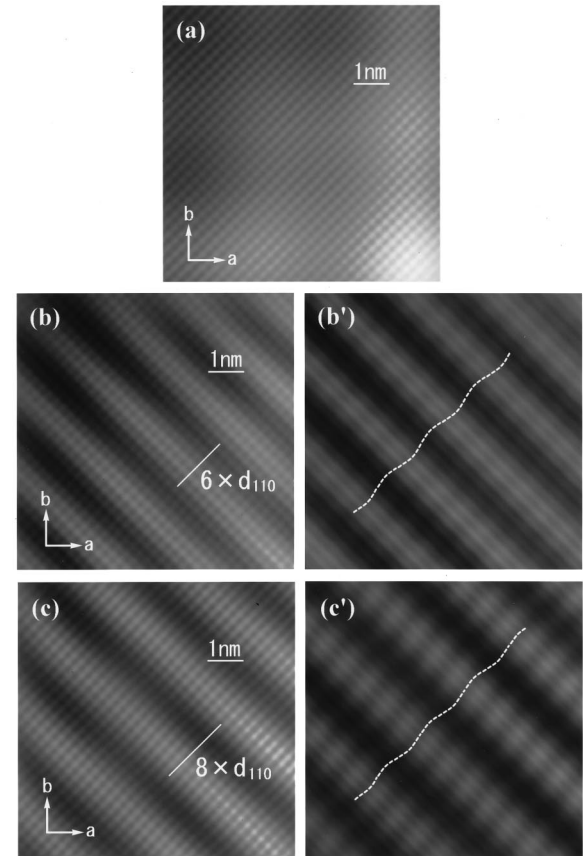


FIG. 3. High-resolution images taken along the [001] direction (a) at 300 K for  $x=2/3$ , (b)–(b′) at 80 K for  $x=2/3$ , and (c)–(c′) at 80 K for  $x=3/4$ . (b′) and (c′) are diagonally (along the  $[1\bar{1}0]$  direction) stretched images. Superlattice fringes and “sinusoidal transverse modulation” of the crystal structure at low temperature are clearly shown.

rection (a) at 300 K for  $x=2/3$ , (b)–(b′) at 80 K for  $x=2/3$ , and (c)–(c′) at 80 K for  $x=3/4$ . [(b′) and (c′) are diagonally stretched images.] Normal  $K_2NiF_4$  structure is shown in the image taken at 300 K ( $>T_{CO}$ ). The images at 80 K ( $<T_{CO}$ ) show clearly superlattice fringes and “transverse modulation” of the crystal structure, with the same period of  $6d_{110}$  ( $x=2/3$ ) or  $8d_{110}$  ( $x=3/4$ ). The observed sinusoidal modulation is in good agreement with invisibility of high-order superlattice reflections in the diffraction patterns (Fig. 1). We propose the structure model given by a sinusoidal transverse modulation on the basis of this observation, and show them in Fig. 4. The transverse displacement is described as  $\Delta y = b_0 \sin(2\pi x_s)$  ( $b_0$ : maximum displacement,  $x_s$ : fractional coordinates along the direction of modulation ( $\mathbf{a}_s$ ) in the superstructure unit cell), where the atoms located at the coordinates of  $x_s=0$  are Mn. The experimentally observed electron diffraction patterns correspond with the simulated ones where  $b_0$  is less than  $\sim 0.03$ . The simulated HREM images also well reproduce the experimentally observed stripe features (Fig. 3). We display in Fig. 5 the images simulated when the crystal is (I) thin: thickness  $t=2$  nm, and (II) thick:  $t=10$  nm. The simulated images when the crystal is thick exhibit superlattice fringes with the

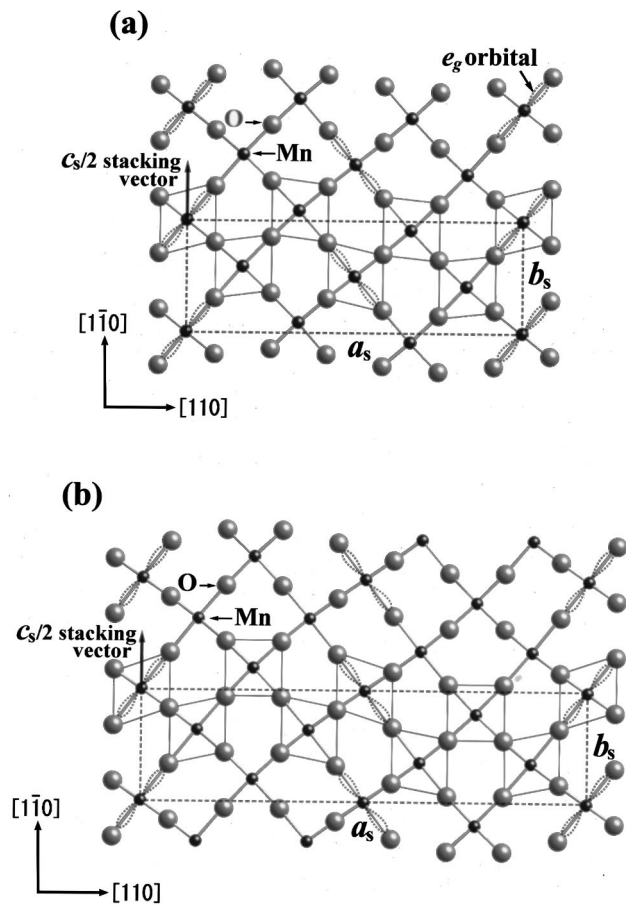


FIG. 4. Proposed superstructure models for (a)  $x=2/3$  and (b)  $x=3/4$ . In order to simplify the drawing, only one of  $\text{MnO}_2$  plane is shown, and the transverse displacement of atoms is exaggerated in the figure. The stacking translation vector along the  $c_s (=c)$  axis in the models is described as  $\mathbf{S} = \mathbf{b}_s/2$ . The space group of the superstructure is  $Acam$  (No. 64) for (a)  $x=2/3$ , and  $Amam$  (No. 63) for (b)  $x=3/4$ .

period of  $6d_{110}$  ( $x=2/3$ ) or  $8d_{110}$  ( $x=3/4$ ), and are almost identical with the experimental ones (Fig. 3). In addition, the simulation study confirmed the sliding of the fringes by varying defocus, which is experimentally observed. It can be seen that  $\text{MnO}_6$  octahedra are most distorted where the central Mn atom is located at the coordinates of  $x_s=0$ , or  $x_s=1/2$  in the proposed models, and that the direction of distortion is different between  $x_s=0$  and  $x_s=1/2$   $\text{MnO}_6$  octahedra; the one direction is at nearly right angles to the other. This significant feature concerning  $\text{MnO}_6$  distortion leads to an agreement between our models and the Wigner-crystal model,<sup>5</sup> where Jahn-Teller-distorted  $\text{Mn}^{3+}\text{O}_6$  stripes are arranged as far apart as possible to minimize the Coulomb repulsion energy. Moreover, in our models, the successive change in the amplitude of  $\text{MnO}_6$  distortion with the position  $x_s$  is suggestive of the modulation of the manganese valence—a CDW of  $e_g$  electrons—or the fluctuation of  $e_g$  electrons around the position of  $x_s=0$  and  $x_s=1/2$ .

Direct observation of transverse modulation in charge-orbital ordered manganite crystals seems to be achieved with the help of the large atomic displacement in the crystals. The

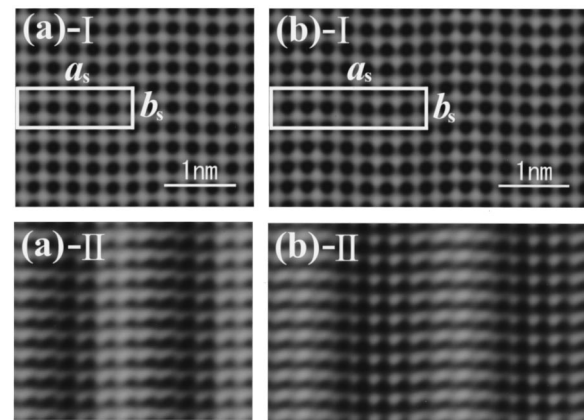


FIG. 5. Simulated HREM images for (a)  $x=2/3$  and (b)  $x=3/4$ , using the proposed superstructure models. The simulations were conducted for the two case, that the crystal is (I) thin: thickness  $t=2$  nm, and (II) thick:  $t=10$  nm. All the simulations were carried out under the condition, defocus:  $\Delta f = -560$  nm and crystal tilt:  $h=k=30$  mrad.

charge-orbital ordered  $\text{Nd}_{1-x}\text{Sr}_{1+x}\text{MnO}_4$  ( $x=2/3, 3/4$ ) crystals give relatively strong superlattice reflection whereas the modulation period is long,  $6d_{110}$  ( $x=2/3$ ) or  $8d_{110}$  ( $x=3/4$ ). The diffraction simulation shows that the intensity of the superlattice reflection increases as the atomic displacement increases. Additionally, the high symmetry of the fundamental structure, tetragonal  $I4/mmm$ , perhaps contributes to the achievement. In three-dimensional perovskites with orthorhombic  $Pnma$  fundamental structure, such as  $\text{La}_{1-x}\text{Ca}_x\text{MnO}_3$ , direct observation of the structural modulation seems to be difficult for tilting of  $\text{MnO}_6$  octahedra.<sup>10</sup>

The observed images indicate that the amplitude of the atomic transverse displacement changes smoothly against the position along the direction of modulation, and that the entire crystal undergoes a sinusoidal transverse modulation. Therefore, we constructed the superstructure model, taking account of the sinusoidal modulation of oxygen atoms as well as cation atoms. Superstructure models which have been proposed by Radaelli *et al.*<sup>4,9</sup> and Wang *et al.*<sup>10</sup> for charge-orbital ordered manganites include an assumption that the amplitude of the displacement of oxygen atom is equal to that of neighboring Mn atom. It should be noted that this sinusoidal modulation of oxygen atoms brings about the aforementioned feature which is not shown in the models proposed by them: modulation of amplitude of  $\text{MnO}_6$  distortion along the direction of superstructure modulation.

In conclusion, we have presented direct observation of the sinusoidal transverse modulation in charge-orbital ordered manganite crystals,  $\text{Nd}_{1-x}\text{Sr}_{1+x}\text{MnO}_4$  ( $x=2/3, 3/4$ ), by high-resolution electron microscopy. The observation and the simulation study support that the charge-orbital ordered state is explained by a Wigner-crystal-type model, which is accompanied with a charge-density wave of  $e_g$  electrons.

The authors would like to thank K. Hatsuda and C. Tsuruta for their collaboration and helpful discussion. This work was supported by the MultiCore Project and Special Coordination Funds of the MEXT, Japan.

- <sup>1</sup>M. Imada, A. Fujimori, and Y. Tokura, *Rev. Mod. Phys.* **70**, 1039 (1998).
- <sup>2</sup>Y. Moritomo, Y. Tomioka, A. Asamitsu, Y. Tokura, and Y. Matsui, *Phys. Rev. B* **51**, 3297 (1995).
- <sup>3</sup>C. H. Chen and S.-W. Cheong, *Phys. Rev. Lett.* **76**, 4042 (1996).
- <sup>4</sup>P. G. Radaelli, D. E. Cox, M. Marezio, and S.-W. Cheong, *Phys. Rev. B* **55**, 3015 (1997).
- <sup>5</sup>C. H. Chen, S.-W. Cheong, and H. Y. Hwang, *J. Appl. Phys.* **81**, 4326 (1997).
- <sup>6</sup>J. Q. Li, Y. Matsui, T. Kimura, and Y. Tokura, *Phys. Rev. B* **57**, R3205 (1998).
- <sup>7</sup>S. Mori, C. H. Chen, and S.-W. Cheong, *Nature (London)* **392**, 473 (1998).
- <sup>8</sup>M. T. Fernandez-Diaz, J. L. Martinez, J. M. Alonso, and E. Herero, *Phys. Rev. B* **59**, 1277 (1999).
- <sup>9</sup>P. G. Radaelli, D. E. Cox, L. Capogna, S.-W. Cheong, and M. Marezio, *Phys. Rev. B* **59**, 14 440 (1999).
- <sup>10</sup>R. Wang, J. Gui, Y. Zhu, and A. R. Moodenbaugh, *Phys. Rev. B* **61**, 11 946 (2000).
- <sup>11</sup>T. Mutou and H. Kontani, *Phys. Rev. Lett.* **83**, 3685 (1999).
- <sup>12</sup>T. Hotta, Y. Takada, H. Koizumi, and E. Dagotto, *Phys. Rev. Lett.* **84**, 2477 (2000).
- <sup>13</sup>T. Kimura, K. Hatsuda, Y. Ueno, R. Kajimoto, H. Mochizuki, H. Yoshizawa, T. Nagai, Y. Matsui, A. Yamazaki, and Y. Tokura, *Phys. Rev. B*. (to be published).
- <sup>14</sup>Y. Murakami, H. Kawada, H. Kawata, M. Tanaka, T. Arima, Y. Moritomo, and Y. Tokura, *Phys. Rev. Lett.* **80**, 1932 (1998).